MEDWIN PUBLISHERS
Committed to create value for Researchers

Nanomedicine & Nanotechnology Open Access
ISSN: 2574-187X

Surface Properties and Morphology of PET Treated by Plasma Immersion Ion Implantation for Food Packaging

Sant'Ana PL[1]*, Ribeiro JR[1], da Cruz NC[1], Rangel EC[1], Durrant SF[1], Costa Botti LM[2], Rodrigues Anjos CA[2], Azevedo S[3], Teixeira V[3], Silval CI[3], Carneiro J[3], Medeiros ÉA[4] and de Fátima Soares NF[4]

[1]Instituto de Ciência e Tecnologia de Sorocaba, State University of São Paulo – UNESP, Brazil

[2]State University of Campinas- UNICAMP, Cidade Universitaria, Brazi

[3]Minho University – UMINHO Largo do Paço s/n Braga, Portugal

[4]Federal University of Viçosa- UFV 36570-000 Campus Viçosa, Brazil

***Corresponding author:** Dr. Péricles Lopes Sant'Ana, PhD, State University of Sao Paulo, UNESP, Av. Três de Março, 511, Alto da Boa Vista, 18087-180 Sorocaba, São Paulo, Brazil, Tel: + 55 15 3018 5130; Email: drsantanapl@gmail.com

Research Article

Volume 3 Issue 3

Received Date: June 02, 2018

Published Date: July 25, 2018

DOI: 10.23880/nnoa-16000145

Abstract

In this work, surface properties of PET (Polyethylene Terephthalate) modified by Plasma Immersion (PI), and Plasma Immersion Ion Implantation (PIII) were studied. Nitrogen and sulfur hexafluoride plasmas were used in a vacuum system coupled to a radiofrequency (rf) generator (13.56 MHz). Infrared spectroscopy (ATR-FTIR) detected the presence of new molecular groups on the PET surface after the treatment. Measurements of the contact angle, θ, revealed a strong dependence of the surface wettability on the plasma parameters, control of which allows the production of hydrophilic or hydrophobic surfaces. The ion fluence was modelled as function of the penetration depth using suitable software (SRIM 2008) and is useful to understand the damage caused by ion implantation of the PET (ρ = 1.39 g/cm^3). The optical transmittance of the treated material in the visible region, T (λ), depends on the gas used and the electrical configuration of the plasma. Water-vapor transmission rate (WVTR) revealed an increase in the barrier properties of the treated PET. PIII technique and N_2 bombardment are more appropriate than plasma immersion and SF_6 bombardment to increase T (λ) of PET in the visible region.

Keywords: PET; PIII; FTIR; Contact angle; SRIM; Barrier Properties

Abbreviations: PET: Polyethylene Terephthalate; PI: Plasma Immersion; PIII: Plasma Immersion Ion Implantation; WVTR: Water-vapor transmission rate.

Introduction

Polymers have wide range of applications in different manufacturing areas, such as food packaging, surgical implants and automobile production. This is mainly due to properties, such as excellent thermal stability, low density and low cost [1]. The low surface energy of polymeric materials, however, negatively affects their use in many applications. This has been remediated using different techniques, such as chemical, thermal or electrical surface treatment [2]. The growing interest in ion-implanted polymeric materials is due to increasing demand in various areas such as optical waveguides, nanocomposites, shielding materials in satellites, space crafts, semiconductors, high energy particle accelerators, etc. [3]. Compared with conventional methods, plasma treatment has many advantages, such as requiring a lower consumption of reagents and energy, producing no waste water, being non-hazardous, dry, fast and environmentally friendly. Moreover, bulk properties are unaffected [4-6]. In addition, it is possible to produce functionalized surfaces using low pressure plasmas. The top 10 to 50 Å of a polymer surface may be altered, without affecting the bulk properties [7]. The study of the induced changes is important for new and advanced technological fields, such as optoelectronics, microelectro nics, filters, electrochemical sensors, medicine, etc. [8]. In this sense, glow discharge plasma-based treatments are of particular interest because they allow surface hydrophilization without producing bulk modifications. However, the instability of the modified surfaces limits their use in many applications [9,10]. Investigations have shown that ions are the most efficient species in the plasma for modifying polymer surfaces. Since the penetration depth of low energy ions in a solid is extremely small, ions seem to be very important for modification of the first few nanometers of the polymer during plasma treatment. Using plasma, one can increase the surface energy of polymeric substrates in an environmentally friendly process without the use of wet chemistry. Plasma activates polymeric surfaces by producing free radicals in the polymeric chain and thus creating new functional groups [11]. There are many techniques that can be used to modify or alter the surface properties of materials by the addition of coatings and functional groups [12,13]. The effects of ion implantation on polymeric materials is of intrinsic scientific interest abut has also attracted attention owing to potential applications in waveguides, shielding materials, etc. [3]. SRIM/TRIM software provides information on the thickness of the modified layer determined by the penetration depth of the ions and their spatial distribution in the polymer matrix. SRIM may also be used to estimate the predicted thickness of implanted layers [14]. The agreement between simulation and experiment is very good in the keV region [15]. Moreover, the flexible substrate materials should meet specific requirements to be integrated to the production of FEDs, such as high optical transparency and high barrier properties against permeation by, for example, oxygen and water vapor. These properties are determined and controlled by the bonding structure of the polymer substrates, the surface nanostructure and chemistry, which controls the functionality of the subsequent functional layers that are developed on the polymer substrates, and finally on the film substrate adhesion [16-18]. Therefore, detailed knowledge of the bonding structure of the samples is necessary. Among the most suitable polymer materials, PET is an excellent material for the production of FEDs, since it is easy to process, has good mechanical properties, and is shows a reasonably high resistance to oxygen and water vapor penetration [19,20]. The evaluation of the water-vapor barrier is also necessary in food packaging applications because many food products are susceptible to humidity [19]. Recent results obtained with PET treated by plasma at low temperature plasma were presented by Nováket [20]. In this work, PIII was used with nitrogen to modify the surface of PET. The aim was to study the effects of PIII on the new chemical surface structures, transparency to visible light, and barrier properties relevant to packaging requirements.

Experimental Procedure

The PET samples were cleaned in an ultrasonic bath (Cristofoli USC 3881) in three steps using: (i) 100 mg detergent DET LIMP S32 + 100 ml deionized water; (ii) 100 ml deionized water; (iii) 100 ml isopropyl alcohol. The experimental setup used consists of a stainless steel vacuum chamber with two internal electrodes [21]. The system was evacuated by a rotary pump (18 m^3/h) down to 10^{-1} Pa. Needle valves were employed to control the gas feeds and a Barocel pressure sensor to monitor the chamber pressure. The total pressure of the reactor was constant at 100 mtorr (13.33 Pa). The temperature during the treatment was maintained at 298 K and the treatment time, t, was 300 s. PET from 2l Coke™ bottles was placed on the stainless steel electrode, and exposed directly to the nitrogen or sulfur hexafluoride plasma environment.

Radiofrequency power (13.56 MHz) of 25 W was applied to the upper electrode; negative pulses at -1000 V and 300 Hz were applied to the lower electrode at cycle times of 1, 30, 100 and 500 μs. Another procedure was achieved when the cycle time was fixed in 30 μs while high voltage was changed from 500 V to 2000 V. The pulsed voltage was monitored by a digital oscilloscope (Tektronix TDS 2014). Effects of the plasma treatment on the chemical composition of the white PET surface were investigated using Attenuated Total Reflection Fourier Transform Infrared Spectroscopy [22,23], FTIR, performed using a Jasco 410 Spectrometer. A similar approach was reported by other authors in previous studies [23,24]. Water contact angle measurements, θ, were obtained immediately after treatment, using a Goniometer (100-00, Rame Hart). The sessile drop technique was employed [25]. Transmittance spectra were obtained in the 190 nm to 3300 nm wavelength range, using a Perkin Elmer spectrometer (Lambda 750 UV-vis-NIR). Water-vapor transmission rate (WVTR) of the PET was determined by following the ASTM gravimetric protocol [26].

Results and Discussions

Infrared Spectroscopy (FTIR)

FTIR is well-established for the elucidation of structural chemical changes [27,28]. Figure 1 (a) shows a spectrum of virgin PET, and (b) shows a spectrum of implanted PET. The N_2 pressure was 13.3 Pa; the applied power 25 W, the treatment time 300s. The cycle time was 30 μs and the applied voltage ranged from -500 V to -2500 V.

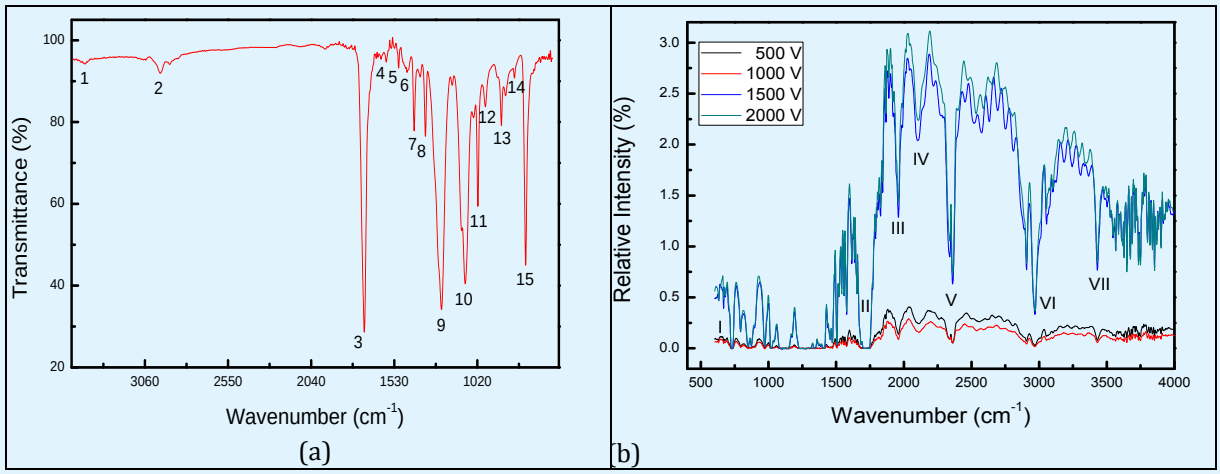

Figure 1: Infrared Spectra of virgin PET for the identification of functional groups in (a) virgin PET (b) implanted PET. The treatment parameters were 13.33 Pa of N_2 for 300 s, at 25 W for different high voltages and a cycle time of 30 μs at 300 Hz.

The following attributions of the observed absorptions were made: Hydrogen on the aromatic ring associated with the band located in 724 cm^{-1} (15), characteristic of out-of-plane vibrations; the presence of $R_2C=CHR$ related to angular deformation of C-H out-of-plane vibration near 792 cm^{-1} (14); and also at 872 cm^{-1} (13) related to the angular deformation of $R_2C=CH_2$; at 970 cm^{-1} (12) related to the angular deformation of -CH=CH- groups; at 1017 cm^{-1} (11) related to S=O (conjugated sulfoxide). An absorption caused by C-O in carboxyl ester groups is observed at 1094 cm^{-1} (10), binding the O-C from the O-CH_2 groups. The band located at 1240 cm^{-1} (9) is caused by the stretching of C=O groups. A band located at 1338 cm^{-1} (8) is associated with the asymmetric angular deformation of sulfone (SO_2). The presence of sulfur-containing groups can indicate the presence of additives in the material or cleaning processes. In addition, more bands were detected, at 1407 cm^{-1} (7), associated with the axial deformation of CH_2; at 1460 cm^{-1} (6) associated with the axial deformation of $-(CH_2)-_n$; at 1504 cm^{-1} (5) associated with the axial deformation of N-H; at 1580 cm^{-1} (4) associated with the symmetric axial in-plane deformation; at 1715 cm^{-1} (3) associated with the C=O bond stretching in the carbonyl group; and also at 2965

cm^{-1} (2), associated with the axial deformation of C-H (stretching), and finally, at 3430 cm^{-1} (1) associated with stretching of the hydroxyl group.

After the ion implantation at low voltages (-500 V and -1000V), weak absorptions were generally observed, while at high voltages (-1500 V and -2000V), absorption increased. The band centers do not shift significantly in wave number. The band observed at 740 cm^{-1} (I) was maintained, associated with the angular deformation of the chain -(CH_2)-n (for n>3), which configures an aromatic ring. The band observed at 1740 cm^{-1} (II) is associated with carbonyl groups. A new group appeared close to 1900 cm^{-1} (III), associated with -C=C=C- alene. This double bond may constitute crosslinking between chains. The origin of another new band, which appears between 2000 and 2200 cm^{-1} (IV), may be SC≡N (thiocyanate), to -N=N=N (azides), or to -C=C=O- (ketones). Unsaturated bonds are present in each of these possibilities. A new band at 2340 cm^{-1} (V) is associated with amine groups. The band near 2965 cm^{-1} (VI) is associated with C=O stretching in carbonyl groups. And finally, the band near 3430 cm^{-1} (VII) is associated with stretching of the hydroxyl group. In all cases, the bands were narrow.

These results are in agreement with recent studies of the plasma treatment of PET [29]. The presence of the new groups after ion implantation explains the hydrophilization of a shallow surface region of the material, by diffusion of water vapor and oxygen from the atmosphere. This diffusion mechanism occurs more intensely in the amorphous regions of the material, or even on the surface on which the atoms have greater mobility. Similar results can be found in current studies [27,28].

Contact Angle Measurements

The contact angle of a liquid on a solid surface, which is closely related to the surface free energy, can be evaluated by means of the sessile drop technique using deionized water at room temperature [30]. Measurement s were made immediately after each plasma treatment. Table 1 shows the contact angle as a function of the cycle time, showing that nitrogen PIII increases hydrophilicity. When the cycle time increases, the water contact angle decreases from 70° on the untreated sample to 19º on the samples treated for 500 μs. Our results are consistent with preview studies, showing that ion bombardment is an effective technique for modification of the surface contact angle [31,32].

PET contact angle (°)	Cycle time (μs)
70.0	0 (untreated)
51.3 ± 1	1
46.0 ± 1	30
31.1 ± 2	100
19.1 ± 1	500

Table 1: Contact angle as a function of the cycle time for PET samples treated with (13.33 Pa) 100 mtorr of N_2 for 300 s, 25 W of RF power for different Ion Implantation cycle times. Pulses of -1000 V at 300 Hz were used.

The table includes Θ values for the condition (-1000 V, 30 μs), that produced new molecular groups (I to VII) according to the FTIR analyses. These groups are probably responsible for the improvement in the wettability. It seems that polar groups formed by the recombination of free radicals contributed to the decrease in the contact angle of PET samples.

Polymer chains have a high degree of flexibility and mobility, which allows the reordering of polar and non-polar groups on the surface of the material through translational and vibrational motion. These processes explain why hydrophilicity also varies with the post-treatment time [33]. Hence, structural changes caused by high energy ions improve the wettability, surface chemical activity, cross-linking and other properties. The structural transformations in the ion-implanted polymers are based on chemical reactions of free radicals which appear as the result of the dangling bonds and displaced target atoms. Reactions occurring in irradiated polymers were considered in a previous publication [34].

Recent studies associated the improvement of wettability with an increase in the concentration of oxygen groups on the PET surface after plasma treatment [35]. The changes in wettability observed after plasma treatment of polymer surfaces after storage of the modified material are explained by mobility of the macromolecules on the top surface level [36]. Accepted models of the surface energy decrease and recovery of hydrophobicity with time in these plasma-treated polymers involve the rotation of high energy surface functional groups back into the polymer bulk. Surface energy is, thereby, reduced and hydrophobicity increased. Such rotations seem unlikely to give the highly carbonized structure associated with high fluence modification. Independently of the efficacy of the treatment, the reduction of Θ, is a transient effect, as observed in [37].

In recent studies, FTIR spectral analyses indicate that the carbon content decreases and the oxygen content increases on the surface of PET, and a large concentration of oxygenated polar functional groups is introduced into the surface by plasma treatment, which is responsible for improving its wettability [38]. Recent studies reveal the wettability issues related to PET. For example, the partial hydrophobic nature of PET results in poor uptake and adhesion of dyes, particles and microcapsules [39].

Plasma Effect on the Polymeric chain and Oxygen Incorporation

Considering that the roughness of the non-treated PET is 1.8 nm, one can see by comparison with the value given in ref [40] that this is a typical value for conventional polymers. It has already been noticed in previous studies that polymers with low roughness respond well to plasma treatment, finding a number of applications, as reported, for example, by Hudis [41]. According to Figure 2, it is possible to observe, for instance, the change of the structure of the polymeric chains after the treatment. Hence, some structural changes were proved by infrared analysis to correlate the improvement in wettability, the increase in roughness, and the changes of optical transmission of the PET samples treated by PIII.

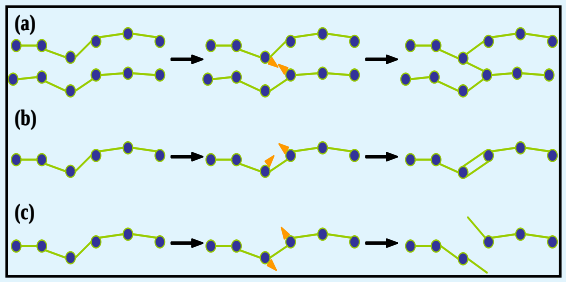

Figure 2: Plasma effects on polymeric chains a due to ionic bombardment: Ion impacts on the carbon backbone cause (a) cross-linking; (b) insaturation. On the other hand, nuclear collisions can dissociate polymeric chains (c) inducing volatile species, which can be removed by the vacuum system.

In one of these studies [42], some polymers, including polyethylenes, were treated with argon and nitrogen plasmas. It was found that nitrogen plasma treatment led to the incorporation of both oxygen and nitrogen functionalities. Plasma immersion, which in turn can be explained by the presence of hydrogen and oxygen incorporated onto the surface, as previously reported, increases the number of species with the same chemical affinity, leading to the formation of hydrogen bonds. To become stable after the treatment, the surface tends to reorient the migration of short chain molecules and the oxidized diffusion of oxidized functional groups into the interior of the material [43].

By the mechanism of oxygen incorporation it is possible to explain the wettability behavior of samples treated with nitrogen. Polymer chains have a high degree of flexibility and mobility that allows the reordering of polar and non-polar groups inside the material through translational and vibrational motion which causes the hydrophobic or hydrophilic character to probably vary depending on the time aging [33]. It is concluded that, as the fluctuations in the values of the contact angle in the aging time can be much smaller for polymers that contain many links cross, they limit the mobility of polymeric chains [44], and therefore; the reorganization of polar groups on the surface is attenued.

Carbon atoms can also be ejected and O addition can be observed. The presence of oxygen in the reactor, either as residual gas or gas released from the glass chamber near the electrode region, may also account for this process. Therefore, the wetting of the bombarded surface is attributed to the electrostatic attraction between dipoles formed by O-containing groups on the PET surface and water molecules in the droplet [45]. In addition, among other effects from the plasma to the polymers during the treatment, plasma consisting of hydrogen, nitrogen and oxygen is used to optimize the radiation of the plasma on the required wavelength ranges based on the results of basic investigations as performed in ref [46-48]. Moreover, the results of plasma sterilization allow for a process time of only 5s, to be in compliance with regulations of FDA [47-49] for aseptic packaging applications.

Therefore, an industrial plasma process can be a good alternative for methods based on toxic chemicals exhibiting major problems, e.g. residues of the sterilants in the package or chemical reactions with the materials [47]. To add or enhance the desired functions, coating processing on polymeric substrates was developed. Since their melting points are considerably lower than those of inorganic materials, low-temperature processing, such as wet coating or plasma deposition, is usually employed. However, adhesion of a deposited layer to a polymeric substrate is not strong enough. Ion implantation technique on polymeric films is an effective means for

solving this delaminating problem and several promising results with ion beam modification on polymeric materials have been reported [50].

SRIM Simulation

The use of ion beams to modify polymer properties opened a wide area of research and utilization in various fields, such as industry, agriculture, ecology, microelectronics and nanotechnology [51,52]. However, the mechanisms responsible for the observed changes are not fully understood. Hence, to analyze the structural changes caused by ion bombardment, a simulation was made using the Stop Range Ions in Matter (SRIM/TRIM Calculation) software. The program was run to associate the changes in surface properties of implanted polymers with the ion-energy loss mechanisms (-dE/dx). The property improvements (mainly attributable to crosslinking) were related to electronic energy transfer (excitation and ionization), and the degradation in properties (as result of scission) to nuclear energy transfer (displacement reactions). When an energetic ion impinges on a polymer, its orbital electrons are stripped off and the nucleus becomes almost naked until the ion velocity slows down below the Bohr electron velocity of the medium [53]. Figure 3, shows respectively, histogram of N_2 atoms penetrating the PET surface at 1 keV, and the range of (a) fluorine and, (b) nitrogen atoms as function of target depth.

It is believed that sulfur hexafluoride treatment promotes F+ ions in plasma, whilst nitrogen treatment promotes N+ ions in plasma. Although the ionization of SF_6 causes SF_x radicals, the software does not recognizes SF_x as input ion data. After irradiation, it is considered that there is a normal distribution of the free radicals with depth.

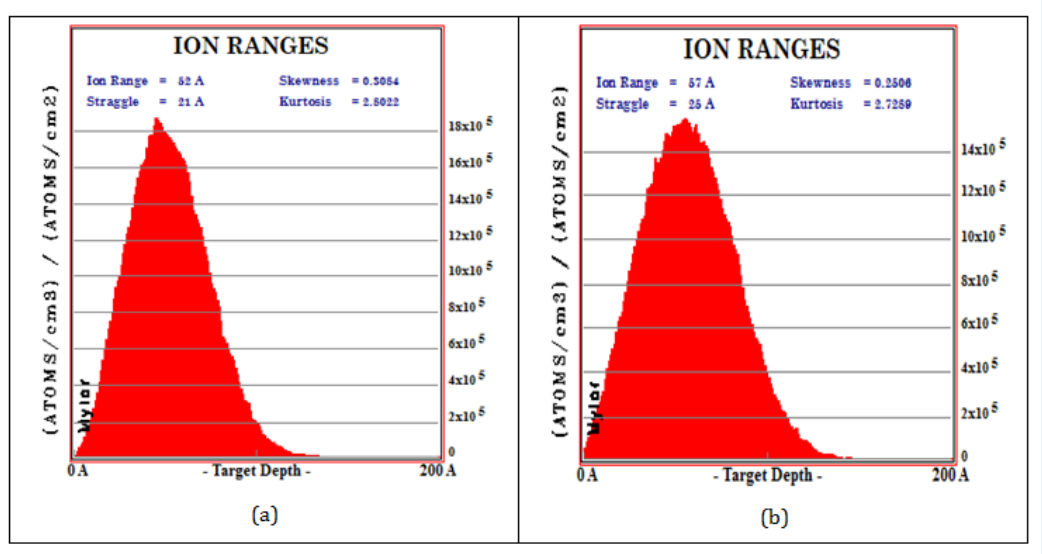

Figure 3: (a) Depth (Angstroms) of incident ions (F^+) for the PET, using incident energy of 1 keV (b) Depth (Angstroms) of incident ions (N^+) for the PET, using incident energy of 1 keV. The histogram represents the range of values average and maximum.

The fluence of atoms (number of ions injected per unit area) as a function of depth depends on the ion kinetic energy and the cycle time. SRIM results indicated a short penetration of ions at low fluence (down to 10^6) distributed in the polymeric matrix, owing to inelastic collisions. The penetration was in the range 0 to ~170 A. A Gaussian curve was used to fit the data.

It is assumed that at the same kinetic energy N^+ ions penetrate more than F^+. Straggling is taken as the mean square root of the variance, being about ~ 0.15 % of the total range of ions penetrating (< 30 angstrom; non-extreme). Considering the PET target as low density material, (ρ = 1.39 g/cm^3), those straggling values are relatively larger, but non-extreme. Skewness presented (dimensionless) positive and small values, thus, indicating

that all the peaks are a bit away from the surface, and the most probable depth is bit smaller than the mean.

After N^+ implantation of the polymer, new functional groups could appear and be located up to a depth of few hundred angstroms. It is suggested that a physical structure on the polymer surface is changed and that seems to be one of the reasons for the enhancement in gas barrier properties in PET bottles [54]. Moreover, The Linear Energy Transfer (LET) was calculated on the basis of nitrogen ion penetration into the PET raw material. Simulating 1 keV of nitrogen ion energy, the maximum ions penetration is less than 200 Angstrom (target depth), owing to the energy loss, which can be estimated by the application of a modified Kinchin-Pease model of recoils [55,56], and a phenomenological model based on formulas from Lindhard, Scharff and Schiott (LSS) and Brandt-Kitagawa theories for electronic stopping [57].

In this process, among other reactions, hydrogen atoms are released from the polymer, and then, cross-linking formation can occur. It has been found that the most important parameter to achieve a high degree of cross-linking is electronic (LET), however, nuclear collisions tends to cause degradation [58]. For the given energy, smaller atoms penetrate deeper and cause fewer nuclear displacements than heavier ones. Experimental results suggest that effective cross-linking occurs when ion pairs in two neighboring chains overlap [59]. According to mean values analyzed, N^+ ions had higher penetrations than F^+.

Ultra Violet Visible Near Infrared Spectroscopy (UV-Vis-NIR)

Figure 4 shows the optical transmittance spectra of PET treated with plasmas of N_2 by PIII. Plasma Immersion Ion Implantation and Plasma Immersion were applied for 300 s at a pressure of 13.33 Pa while the applied radio frequency power was 25 W. The pulsed voltage was -1040 V at 300 Hz, while the cycle time was changed from 1, 30, 100 and 500 μs and the temperature was maintained at 298 K. As a general trend, it is possible to observe that the transmittance remains almost constant in the visible wavelength range (400-700 nm) and progressively decreases for λ below 400 nm. No great differences are observed in the spectra of the untreated and treated samples.

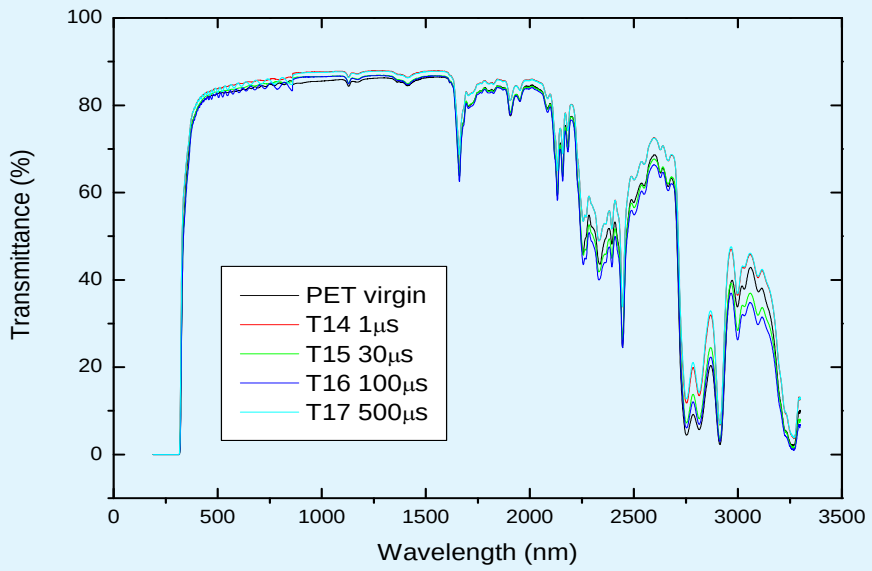

Figure 4: Optical transmittance as a function of the wavelength of PET samples treated with 13.33 Pa of N_2 for 300 s, at 25 W for different cycle times. The pulsed voltage was -1040 V at 300 Hz.

For many applications, transparent materials are sought to allow a clear vision of the product. From a practical point of view, the "see-through" property, which is obtained by reducing the contrast between objects viewed through the material, is actually one of the most important requirements as it can influence the final

choice made by consumers [60]. For opto-electronic applications, the transparent substrates must be able to maintain their high optical transparency after high temperature heating, caused by plasma processes. This is a serious issue for flexible polymer substrates. Polyethylene terephthalate (PET) films are colorless, transparent (refractive index = 1.8564), and low cost, but do not have enough thermal durability for the above-mentioned high temperature process [61]. In this same study, a high transmittance (close to 89%) and low reflection (4.5 %) were measured for PET. The procedure used in the present study avoids loss of transparency caused by high temperatures.

Analyzing Figure 4 reveals that the optical transmittance tends to increase with increasing cycle time. This may be caused by a decrease in reflectance. A reduction in roughness of PET samples implanted with nitrogen plasmas may be responsible for this decrease. The values of roughness for PET implanted with nitrogen plasmas were observed in Sant'Ana (2014) [27]. Strong absorption of carbonyl groups and its derivatives, occur in the range from 200 nm to 350 nm [62], which explains the very low transmittance in this range. Analogously, higher surface roughness (2.1 nm < Rrms < 16.7 nm) found for treated PET decreased T (λ), due to optical scattering caused by rough surface morphology [63]. In agreement with other studies, it was found that the decrease in PET transparency correlates with the increase in roughness [64]. The spectra of samples in the range of wavenumber from 650 to 1000 cm^{-1} show bands very well studied in the literature for the characterization of PET [65,66]. According Manley and Williams, the intensity of these bands is moderately independent of the surface roughness of the target material [67].

Water Vapor Barrier Properties

The evaluation of the water-vapor barrier is necessary because many food products are susceptible to humidity [20]. Therefore the water-vapor transmission rate (WVTR) of the PET was determined by the gravimetric method, according to ASTM [26], at a humidity of 75 % humidity and a room temperature of 24 ± 1ºC. The results are presented in Table 2. Thickness of the PET did not demonstrate significant differences ($p > 0.05$) among the treatments.

Plasma Parameters	Thickness (mm)	WVTR (g/m² day)	(σ)
Virgin PET	0.050	6.12	0.33
PI 25W 300 s	0.050	0.91	0.19
PI 100W 300 s	0.049	1.04	0.27
PI 25W 600 s	0.049	0.95	0.20
PI 100W 600 s	0.048	0.99	0.17
PI 150W 900 s	0.048	0.93	0.24
PIII 25W 300 s -500 V	0.062	1.05	0.35
PIII 25W 300 s -1000 V	0.048	1.05	0.17
PIII 25W 300 s -1500 V	0.049	0.88	0.11

Table 2: Water-vapor transmission rate of PET samples treated with nitrogen plasmas under different conditions.

The use of plastic materials for flexible food packaging also poses a challenge in finding appropriate strategies to improve their barrier properties [68]. Among rigid containers used in the food and beverage industry, PET bottles are the most widely studied plastic containers for gas barrier enhancement because of their industrial scale use. It should be stressed that the demand for high gas barrier PET bottles has been increasing because of the global trend in weight reduction, where thinner bottle walls show poorer gas barrier performance [69], and of a gradual increase of the applications of PET bottle formats, as reported in recent studies [70]. The results found in our studies are characteristic of high barrier material, normally associated with laminated films, opaque composites of various substrates, which may or may not contain aluminum foil or other metalized layers to improve the material properties [71]. The results of this work are in agreement with studies of plasma deposition in polymeric films as observed by Bieder (2005), and confirmed by [72-74] Czeremuszkin, et al. (2001). Garcia, et al. (1996) and Henry (1999), managed to improve the barrier property of materials treated by reducing the values of WVTR of films 150 times.

In one study, starch films containing 2% glycerol and 0.0% chitosan showed a higher permeability to water vapor compared to other films [75]. The absence of chitosan in the film may have enabled a greater

plasticizing action of the glycerol molecule in the starch polymer chains, thereby increasing the permeability to water vapor. Furthermore, the hydrophilic character of glycerol favors the absorption and desorption of water molecules, as reported by Mali, et al. [76]. One of the suggestions for the completion of the investigation in this line of research is the treatment of plasma films containing starch or acetate, or other sugars, to give the treated packaging selective surface properties.

Although treatment affects only a very thin layer in comparison to 'bulk', it is believed that, for the samples of the PET investigated, the processing plasma can be sufficient to promote the closing of the matrix, stimulated by unsaturation processes and anchor points, which are inherent condition effects. In fact, one of the effect of plasma treatment on polymers is to promote the formation of double bonds and anchor points, which approximates adjacent chains, causing entanglements. It is worth pointing out the best condition was noted for PIII at -1500 V, which presented the small WVTR (0.88 g/m^2 day). Also, plasma treatment may fill voids contained in the structure of the polymer chains. Another advantage is related to our procedure that fixed the temperature of the substrates (25ºC) during the treatment. In this way, it is possible to stay below the glass transition temperature, and retain the high optical transmittance of the PET substrates in the visible range. The glass transition temperature for PET is about 60 to70ºC [77].

Conclusions

Plasma treatment has been effective to improve the surface properties of PET samples. FTIR indicates the presence of new unsaturated (double or triple) bonds. Both atoms and ions have a role in the modification of the treated material. The plasma contains C, O, N, and H atoms, which usually create polar radicals and O containing groups. Thus, the surface contact angle Θ, decreased owing to the chemical affinity of polar groups formed on the surface, and water molecules. Therefore surface wettability was increased. Modelling of the depth profile of the implanted ions shows a Gaussian distribution. In this case, the degree of deviation or scattering of these ions occurs randomly. Plasma treatment produced cross-linking in the PET surface, thereby improving gas barrier properties under all treatment conditions studied. Optical transparency was not reduced by the treatments.

Acknowledgements

The authors thank the Brazilian agencies CAPES, CNPQ, and FAPESP for financial support.

References

1. Shaw D, Gyuk P, West A, Momoh M, Wagenaars E (2015) Surface Modification of Polymer Films Using an Atmospheric-Pressure Plasma Jet. In Proc 22nd ISPC, York.

2. Subedi DP, Baniya HB, Shrestha R, Shrestha A, Shrestha S, et al. (2014) Surface Modification of Polycarbonate by Atmospheric Pressure Cold Argon/Air Plasma Jet. Journal of science Engineering and technology 10(2): 13-16.

3. Goorsky M (2012) Ion Implantation, In Tech Publisher, Croatia, pp: 448.

4. Li G, Liu H, Li T, Wang J (2012) Surface modification and functionalization of silk fibroin fibers/fabric toward high performance applications. Materials Science and Engineering C 32(4): 627-636.

5. Gogoi D, Choudhury AJ, Chutia J, Das NN, Pal AR, et al. (2011) Enhancement of hydrophobicity and tensile strength of muga silk fiber by radiofrequency Ar plasma discharge. Applied Surface Science 258(1): 126-135.

6. Sargunami D, Selvakumar N (2006) A study on the effects of ozone treatment on the properties of raw and degummed mulberry silk fabrics. Polymer Degradation and Stability 91(11): 2644-2653.

7. Aflori M, Drobotă M, Ţîmpu D, Bărboiu V (2007) Amine functionality of poly(ethylene terepthalate) films surfaces induced by chemical and RF plasma treatments, 28th Int Conf Phenom Ion Gases Prague, pp: 727-730.

8. Shekhawat N, Aggarwal S, Sharma A, Nair KGM (2016) N+ Implantation-Induced Surface Hardening of Poly (Allyl Diglycol Carbonate) Polymer. J Macromol Sci Part B Phys 55(7): 652-661.

9. Banik I, Kim KS, Yun YI, Kim DH, Ryu CM, et al. (2002) Inhibition of aging in plasma-treated high-density polyethylene. J Adhes Sci Technol 16(9): 1155-1169.

10. Larsson A, Derand H (2002) Stability of Polycarbonate and Polystyrene Surfaces after Hydrophilization with High Intensity Oxygen RF Plasma. J Colloid Interface Sci 246(1): 214-221.

11. Huang C, Ching-Yuan T, Ruey-Shin J (2012) Surface Modification and Characterization of an H_2/O_2 Plasma-Treated Polypropylene Membrane. Journal of Applied Polymer Science 124(1): 108-115.

12. Rabies A, Shandukas S (2013) Processing and evaluation of bioactive coatings on polymeric implants. Journal of Biomedical Materials Research Part A 101(9): 2621-2629.

13. Hahn BD, Park DS, Choi JJ, Ryu J, Yoon WH, et al. (2013) Osteoconductive hydroxyapatite coated PEEK for spinal fusion surgery. Applied Surf ace Science 283: 6-11.

14. Kavetskyy TS, Stepanov AL (2015) Spectroscopic investigations of ion-induced processes in polymethylmethacrylate at low-energy boron-ion implantation. In: Proceedings of the XXII International Conference on Ion-Surface Interactions. NRNU MEPh I, Moscow, pp: 339-342.

15. Fink D (2004) Fundamentals of íon-irradiated polymer. Springer Series in Material Science, Berlin.

16. Logothetidis S (2005) Polymeric Substrates and Encapsulations for Flexible Electronics: Bonding Structures Surface Modification and Functional Nanolayer Growth. Rev Adv Mater Sci 10(5): 387-397.

17. Hanika M, Langowski HC, Moosheimer U, Peukert W (2003) Inorganic Layers on Polymeric Films – Influence of Defects and Morphology on Barrier Properties. Chem Eng Technol 26(5): 605-614.

18. Laskarakis A, Logothetidis S (2006) On the optical anisotropy of poly(ethylene terephthalate) and poly(ethylene naphthalate) polymeric films by spectroscopic ellipsometry from visible-far ultraviolet to infrared spectral regions. J Appl Phys 99(6): 066101.

19. Michael D, Helmut H, Simon S, Nikita B, Peter A (2009) Silicon Oxide Permeation Barrier Coating and Plasma Sterelization of PET Bottles and Foils. Plasma Processes and Polymers 6(1): 695-699.

20. Novák I, Chodák I, Sedlia_Ik J, Števiar M, Popelka A, et al. (2010) Investigation of poly(ethylene terephthalate) treated by low-temperature plasma. Annals of Warsaw University of Life Sciences –SGGW Forestry and Wood Technology 72: 83-89.

21. Mojab CJ (1980) Glow Discharge Processes by Brian Chapman. Journal of Vacuum Science & Technology A Vacuum Surfaces and Films 19(3): 812.

22. Fowkes FM (1987) Role of acid-base interfacial bonding in adhesion. J Adhesion Sci Technol 1(1): 7-27.

23. Barbosa LCA (2007) Espectroscopia no infravermelho na caracterização de compostos orgânicos. Viçosa: Ed UFV (1):189.

24. Agnelli JAM (1992) Caracterização de Polímeros por Espectroscopia no Infravermelho. Apostila da Associação Brasileira de Polímeros 1: 61.

25. John M Casper (1976) Physical Chemistry of Surfaces, Arthur W Adamson, Wiley-Interscience, New York, pp: 698 pp.

26. Kumaran M (1998) Interlaboratory Comparison of the ASTM Standard Test Methods for Water Vapor Transmission of Materials. Journal of Testing and Evaluation 26(2): 83-88.

27. Sant'Ana, Péricles Lopes (2014) Plásticos comerciais tratados a plasma para dispositivos ópticos e embalagens alimentícias, f. Tese (doutorado) - Universidade Estadual Paulista Julio de Mesquita Filho, Faculdade de Ciências.

28. Sant'Ana PL, Bortoleto JRR, Nilson C Cruz, Elidiane C Rangel, Durrant SF (2017) Study of Wettability and Optical Transparency of PET Polymer modified by Plasma Immersion Ion Implantation techniques. Revista Brasileira de Aplicações de Vácuo 36(2): 68-74.

29. Drobota M, Aflori M, Barboiu V (2010) Protein Immobilization on poly (ethylene terephthalate) films modified by plasma and chemical treatments. Digest Journal of Nanomaterials and Biostructures 5(1): 35-42.

30. Kim Y, Lee Y, Han S, Kim KJ (2006) Improvement of hydrophobic properties of polymer surfaces by

plasma source ion implantation. Surf Coat Technol 200(16/17): 4763-4769.

31. Chassé M, Ross GG (2002) Modification of wetting properties of SiO_x surfaces by Ar implantation. Nucl Instrum Methods Phys Res B Beam Interact Mater 193(1-4): 835-845.

32. Rupp F, Scheideler L, Rehbein D, Axmann D, Geis-Gerstorfer J (2004) Roughness induced dynamic changes of wettability of acid etched titanium implant modifications. Biomaterials 25(7/8): 1429-1438.

33. Darbello SM (2008) Estudo da reciclagem mecânica de Poli (Cloreto de Vinila) PVC proveniente de resíduos da construção civil. Dissertação de Mestrado UNESP/Sorocaba. Universidade Estadual Paulista, Faculdade de Ciência de Bauru.

34. Kondyurin A, Bilek M (2008) Ion beam treatment of polymers. Oxford: Elsevier, pp: 327.

35. Resnik M, Zaplotnik R, Mozetic M, Vesel A (2018) Comparison of SF_6 and CF_4 Plasma Treatment for Surface Hydrophobization of PET Polymer. Materials 11(2): 311.

36. Yasuda H (2005) Luminous chemical vapor deposition and interface engineering, Marcel Dekker Surfactant Science Series, pp: 840.

37. Rangel EC, Gadioli GZ, Cruz NC (2004) Investigations on the Stability of Plasma Modified Silicone Surfaces. Plasmas and Polymers 9(1): 35-48.

38. Akishev YS, Grushin ME, Drachev AI, Karalnik VB, Petryakov AV, et al. (2013) On Hydrophilicity Ageing of PP and PET Films Induced by Ultraviolet Radiation and Hydrogen Atoms. The Open Plasma Physics Journal 6: 19-29.

39. Al-Etaibi A, Alnassar H, El-Apasery M (2016) Dyeing of polyester with disperse dyes: Part 2. Synthesis and dyeing characteristics of some azo disperse dyes for polyester fabrics, Molecules 21(7): 855.

40. He XM, Walter KC, Nastasi M, Lee ST, Sun XS (1999) Optical and tribological properties of diamond-like carbon films synthesized by plasma immersion ion processing. Thin Solid Films 355-356(1): 167-173.

41. Eli Pearce (1975) Techniques and applications of plasma chemistry. In: John R Hollahan and Alexis T Bell (Eds., John Wiley & Sons, New York. Journal of Polymer Science Polymer Letters 13(1): 59-60.

42. Yasuda H, Marsh HC, Brandt ES, Reilley CN (1977) ESCA study of polymer surfaces treated by plasma. J Polym Sci Polym Chem 15(4): 991-1019.

43. Foerch R, Kill G, Walzak MJ (1993) Plasma Surface Modification of Polypropylene: Shortterm vs. Long-term Plasma treatment. Journal of Adhesion Science and Technology 7(10): 1077-1089.

44. Sadeek SA (2005) Synthesis, thermogravimetric analysis, infrared, electronic and mass spectra of Mn(II), Co(II) and Fe(III) norfloxacin complexes. J Molec Struct 753(1-3): 1-12.

45. Roger Parsons (1976) Physical Chemistry of Surfaces by Arthur W Adamson, Wiley, New York, pp: 698.

46. Halfmann H, Bibinov N, Wunderlich J, Awakowicz P (2007) Identification of the most efficient VUV/UV radiation for plasma based inactivation of Bacillus atrophaeus spores. J Phys D Appl Phys 40(19): 5907-5911.

47. Halfmann H, Bibinov N, Wunderlich J, Awakowicz P (2007) Correlation between VUV radiation and sterilization efficiency in a double inductively coupled plasma. Proceedings of the XXVIII International Conference on Phenomena in Ionized Gases (ICPIG) 28(16): 1382-1384.

48. Halfmann H (2008) Characterization of Low Pressure Double Inductively Coupled Plasma, Determination of Fundamental Sterilization Mechanisms and Surface Modification of Medical Materials. PhD Thesis, Ruhr-Universitat Bochum, pp: 120.

49. Ocasio WC (2005) The Opacity of Risk: Language and the Culture of Safety in NASA's Space Shuttle Program. In: Farjoun M & Starbuck WH (Eds.), Organization at the Limit: Management Lessons from the Columbia Disaster Blackwell, pp: 409.

50. Benz D, Irausquin H (1991) Priority-Based Assessment of Food Additives Database of the US Food and Drug Administration Center for Food Safety and Applied Nutrition. Environ Health Perspect 96: 85-89.

51. Girolamo GD (2012) Strain gauges fabricated by C+ ion implantation in bulk polymers. Sensors and Actuators A 178: 136-140.

52. Abdul-Kader AM, El-Badry BA, Zaki MF, Hegazy TM, Hashem HM (2010) Ion beam modification of surface properties of CR-39. Philos Mag 90(19): 2543-2555.

53. Suzuki Y, Kusakabe M, Akiba H, Kusakabe K, Iwaki M (1991) In vivo evaluation of antithrombogenicity for ion implanted silicone rubber using indium-111-tropolone platelets. Nucl Instr Meth B 59-60(1): 698-704.

54. Sioshansi P (1987) Medical application of ion beam processes. Nucl Intr and Meth B 19-12(1): 204-208.

55. Lee EH, Rao GR, Mansur LK (1996) Super-hard-surfaced Polymers by High-energy Ion-beam Irradiation. Trends in Polymer Science 4(7): 229-237.

56. Okuji S, Sekyia M, Nakabayashi M, Endo H, Sakudo N, et al. (2006) Surface modification of polymeric substrates by plasma-based ion implantation. Nuclear Instruments and Methods in Physics Research B 242(1-2): 353-356.

57. Sigmund P (1969) A note on integral equations of the kinchin-pease type. Radiat Eff 1(1): 15-18.

58. Norgett MJ, Torrens IM, Robinson MT (1974) A proposed method of calculating displacement dose rates. Nucl Eng Des 33(1): 50-54.

59. Ziegler JF, Biersack JP, Littmark U (1985) The Stopping and Range of Ions in Solids. Pergamon Press 1: 321.

60. Introzzi L, Fuentes-Alventosa JM, Cozzolino CA, Trabattoni S, Tavazzi S, et al. (2012) 'Wetting enhancer' pullulan coating for anti-fog packaging applications. ACS Appl Mater Interfaces 4(7): 3692-3700.

61. Nogi M, Kim C, Sugahara T, Inui T, Takahashi T, et al. (2013) High termal stability of optical transparency in cellulose nanofiber paper. Applied Physics Letters 102(18): 181911.

62. Field LD, Sternhell S, Kalman JR (2008) Organic Structures from Spectra. Concepts in Magnetic Resonance Part A 32(5): 405-406.

63. Tho SY, Ibrahim K (2012) Influence of Surface Roughness of Polyethylene Terephthalate (PET) Substrate to the Morphology and Optical Properties of Coated Zinc Oxide Thin-film. Jurnal Teknologi 59(3): 5-8.

64. Larena A, Millán F, Pérez G, Pinto G (2002) Effect of surface roughness on the optical properties of multilayer polymer films. Applied Surface Science 187(3-4): 339-346.

65. Yazdanian M, Ward IM, Brody H (1985) An infra-red study of the structure of oriented poly(ethylene terephthalate) fibres. Polymer 26(12): 1779-1790.

66. Quintanilla L, Rodríguez-Cabello JC, Tawhari T, Pastor JM (1993) Structural analysis of injection-moulded semicrystalline polymers by Fourier transform infra-red spectroscopy with photoacoustic detection and differential scanning calorimetry: 1. Poly(ethylene terephthalate). Polymer 34(18): 3787-3795.

67. Manley TR, Williams DA (1969) Structure of terephthalate polymers I-Infra-red spectra and molecular structure of poly (ethylene terephthalate). Polymer 10: 339-384.

68. Fei Li, Paolo Biagioni, Monica Bollani, Maccagnan A, Piergiovanni L (2013) Multi-functional coating of cellulose nanocrystals for flexible packaging applications. Cellulose 20(5): 2491-2504.

69. Shirakura A, Nakaya M, Koga Y, Kodama H, Hasebe T, et al. (2006) Diamond-like carbon films for PET bottles and medical applications. Thin Solid Films 494(1-2): 84-91.

70. Nakaya M, Uedono A, Hotta A (2015) Recent Progress in Gas Barrier Thin Film Coatings on PET Bottles in Food and Beverage Applications. Coatings 5(4): 987-1001.

71. Alves RMV, Minalez CR, Padula M (2000) Cappuccino in flexible packaging. Anais Sbicafe: 654-657.

72. Czeremuskin G, Latrèche M, Wertheimer MR, da Silva Sobrinho AS (2001) Ultrathin Silicon compound barrier coatings for polymeric packaging materials: an industrial perspective. Plasmas Polym 6(1-2): 107-120.

73. Garcia Ayuso G, Vazquez L, Marinez Duart JM (1996) Atomic Force Microscopy (AFM) Morphological

Surface Characterization of of Transparent Gas Barrier Coatings on Plastic Films. Surf Coat Technol 80(1-2): 203-206.

74. Henry BM, Dinelli F, Zhao KY, MGrovenor CR, Kolosov OV, et al. (1999) A microstructural study of transparent metal oxide gas barrier films. Thin Solid Films 355-356: 500-505.

75. De Paula CD, Pirozi M, Puiatti M, Borges JT, Durango AM (2012) Physicochemical and Morphologic Characteristics of the Rizóforos of Yam (Dioscorea alata). Rev Bio Agro 10(2): 61-70.

76. Mali S, Grossmann M, García M, Martino M, Zaritzky N (2004) Barrier, mechanical and optical properties of plasticized yam starch films. Carbohydrate Polymers 56(2): 129-135.

77. Auras R, Harte B, Selke S (2004) An overview of polylactides as packaging materials. Macromol Biosci 4(9): 835-864.